Centrifuge Permeameter for Unsaturated Soils. II: Measurement of the Hydraulic Characteristics of an Unsaturated Clay

John S. McCartney, A.M.ASCE[1]; and Jorge G. Zornberg, M.ASCE[2]

Abstract: This paper presents the hydraulic characteristics of an unsaturated, compacted clay, including its soil-water retention curve (SWRC) and hydraulic conductivity function (K function), determined using a new centrifuge permeameter developed at the University of Texas at Austin. A companion paper describes the apparatus, its instrumentation layout, and data reduction procedures. Three approaches are evaluated in this study to define the SWRC and K function of the compacted clay under both drying and wetting paths, by varying the inflow rate, the g level, or both. For imposed inflow rates ranging from 20 to 0.1 mL/h and g levels ranging from 10 to 100 g, the measured matric suction ranged from 5 to 70 kPa, the average volumetric water content ranged from 23 to 33%, and the hydraulic conductivity ranged from 2×10^{-7} to 8×10^{-11} m/s. The SWRCs and K functions obtained using the three different testing approaches were very consistent, and yielded suitable information for direct determination of the hydraulic characteristics. The approaches differed in the time required to complete a testing stage and in the range of measured hydraulic conductivity values. The g level had a negligible effect on the measured hydraulic characteristics of the compacted clay. The SWRCs and K functions defined using the centrifuge permeameter are consistent with those obtained using pressure chamber and column infiltration tests. The K functions defined using the centrifuge permeameter follow the same shape as those obtained from predictive relationships, although the measured and predicted K functions differ by two orders of magnitude at the lower end of the volumetric water content range.

DOI: 10.1061/(ASCE)GT.1943-5606.0000320

CE Database subject headings: Centrifuge; Unsaturated soils; Hydraulic conductivity; Soil water; Clays.

Author keywords: Centrifuge permeameter; Unsaturated soils; Hydraulic conductivity function; Soil water retention curve.

Introduction

Zornberg and McCartney (2010) presented the details of a new centrifuge permeameter, along with the theoretical basis for determination of the hydraulic characteristics of unsaturated soils, including the soil-water retention curve (SWRC) and hydraulic conductivity function (K function). An important advantage of the new equipment over previous centrifuge permeameters such as the steady-state centrifuge (SSC) apparatus (Nimmo 1987) and the unsaturated flow apparatus (Conca and Wright 1992) is that it includes a fully functional data acquisition system for in-flight monitoring. Accordingly, instrumentation can be used to measure changes in discharge velocity v_m, volumetric water content θ, and matric suction ψ during centrifugation. Specifically, the discharge velocity is inferred by a pressure transducer used to measure the outflow volume collected with time, the average volumetric water content in the soil is obtained using a time domain reflectometry (TDR) waveguide embedded in the permeameter sidewall, and the ψ profile along the specimen height is measured using an array of three tensiometers embedded into the permeameter sidewall.

A schematic view of the centrifuge permeameter, including the locations of the different instruments, is shown in Fig. 1. Consistent with the current ASTM standard for determination of the K of unsaturated soils in a centrifuge [ASTM D6527 (ASTM 2000)], steady-state infiltration is used in this study in order to allow direct calculation of K. An infusion pump (located outside of the centrifuge) and a low-flow rotary joint are used to supply a constant inflow rate Q to the specimen, independent of the centrifuge angular velocity ω. A fluid distribution system is used to permit free movement of air into or out of the specimen during infiltration.

The objectives of this paper are to present the determination of hydraulic characteristics of unsaturated soils using a centrifuge permeameter, and to compare the hydraulic characteristics obtained from the centrifuge permeameter with those obtained using conventional tests and from predictive relationships. Specifically, this paper presents the instrumentation results from a steady-state infiltration test performed on a single specimen in the centrifuge permeameter, conducted to define the wetting and drying portions of the SWRC and K function of compacted clay of low plasticity. The results obtained from this test also allow assessment of the advantages and disadvantages of various testing approaches, which incorporate different strategies to control the inflow rate and centrifuge speed.

[1]Barry Faculty Fellow and Assistant Professor, Dept. of Civil, Environmental, Architectural Engineering, Univ. of Colorado at Boulder, UCB 428, Boulder, CO 80302 (corresponding author). E-mail: john.mccartney@colorado.edu

[2]Fluor Centennial Associate Professor, Department of Civil Engineering, Geotechnical Group, the Univ. of Texas at Austin, 1 Univ. Station, C1792, Austin, TX 78712-0280. E-mail: zornberg@mail.utexas.edu

Note. This manuscript was submitted on December 24, 2008; approved on December 24, 2009; published online on January 8, 2010. Discussion period open until January 1, 2011; separate discussions must be submitted for individual papers. This paper is part of the ***Journal of Geotechnical and Geoenvironmental Engineering***, Vol. 136, No. 8, August 1, 2010. ©ASCE, ISSN 1090-0241/2010/8-1064–1076/$25.00.

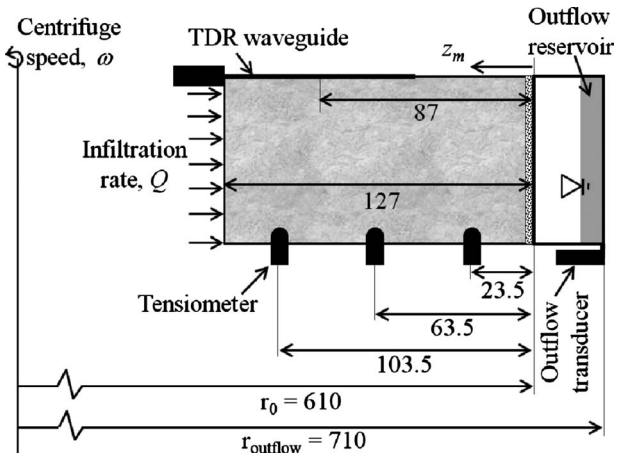

Fig. 1. Schematic showing the centrifuge permeameter geometry and instrumentation locations (dimensions in millimeters)

Materials

Although a centrifuge approach can be used for a variety of soils, the conditions under which a given soil should be investigated in the centrifuge depends on the stresses associated with the centrifuge acceleration field, the testing time required for hydraulic characterization, the ability of the centrifuge system to achieve the desired values of g level and a uniform rate of infiltration, and the functionality of instrumentation used to measure θ and ψ. Some mechanical and hydraulic characteristics of soil that also may affect the ability to conduct a centrifuge permeameter testing include its compressibility under unsaturated and saturated conditions, its tendency to swell or shrink upon changes in volumetric water content, and the range in K, θ, and ψ that can be achieved with the selected flow pump and instrumentation.

The hydraulic characteristics of remolded and compacted clay specimens were investigated in this study. Specifically, the soil used in this study is a clay of low plasticity, classified as CL according to the Unified Soil Classification System. The soil was obtained from test cover plots constructed as part of the alternative cover demonstration at the Rocky Mountain Arsenal near Denver, Colorado. The granulometric curve for the soil is shown in Fig. 2(a). The percentage of fines in the soil is approximately 68%. The specific gravity of the solids was determined to be 2.7, the soil has a liquid limit of 29 and a plasticity index of 17.

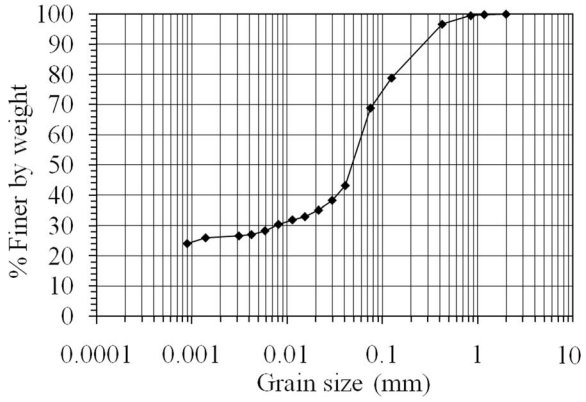

Fig. 2. Granulometric curve for the clay of low plasticity evaluated in this study

This soil is well suited for characterization using the centrifuge permeameter. Specifically, the compacted clay is relatively stiff and has a relatively low compressibility. Accordingly, there are no perceived restrictions on the centrifuge speeds that can be used for characterization, although only g levels below 100 g were used in this study. The saturated hydraulic conductivity K_s of the compacted clay ranges from 10^{-4} m/s at a porosity of 50% to 10^{-9} m/s at a porosity of 27% (McCartney 2007). This range of K_s is consistent with the inflow rate that can be imposed by the infusion pump adopted by this study. Also, good distribution of infiltration across the area of the specimen was observed for this range of infiltration rates. The clay has low salinity and electrical conductivity, permitting the use of dielectric sensors to infer θ. For the soil used in this investigation, the test conditions were only limited by the flow rate that could be imposed by the selected flow pump and by the range of ψ values that could be measured with the selected ψ measurement devices.

The centrifuge permeameter can simultaneously spin two soil specimens with approximately identical masses. Accordingly, two specimens of the clay were prepared using kneading compaction in two identical permeameters, referred to as Permeameters A and B. The specimens were prepared to reach a target dry density of 1,710 kg/m^3, which is 90% of the maximum dry density corresponding to the standard Proctor compaction effort ($\gamma_{d,\max}$ = 1,900 kg/m^3). The compaction water content for both specimens was the optimal gravimetric water content (11.8%). After compaction, the porosity values of the specimens in Permeameters A and B were found to be 34.5 and 34.9%, respectively, with an initial degree of saturation of 0.6. The value of K_s corresponding to these compaction conditions was measured for a third soil specimen, prepared using identical conditions (to a porosity of 34.6%) in a split-wall mold. A K_s value of 1.2×10^{-7} m/s was obtained for an effective confining pressure of 20 kPa and a gradient of 1.5. After compaction, the permeameters were placed into the centrifuge, tensiometers were attached, and the inflow distribution system was assembled. The tests evaluated in this study were started from near-saturated conditions, although this is not necessary in a general application of this test method. Specifically, moisture conditioning procedures involved wetting the specimens by ponding water atop the specimens in the permeameters while simultaneously placing the base of the permeameter in a water bath for 2 days before centrifugation. TDR measurements made after the initial saturation phase indicate a degree of saturation in both specimens of approximately 0.9. More details about the compaction and assembly procedures of the centrifuge permeameter system are given in McCartney (2007) and Zornberg and McCartney (2010).

Experimental Procedures

The inflow rate Q and centrifuge speed ω are the primary variables that can be controlled in the centrifuge permeameter while conducting an infiltration test. Consequently, Q and ω are referred to as control variables. The protocol for centrifuge permeameter testing involves selecting a combination of control variables, and imposing them to the centrifuge permeameter until steady-state water flow is attained in the soil specimens. The variables that should be measured in the centrifuge permeameter to define the SWRC and K function include the discharge velocity (to ensure that a steady-state condition has been attained) as well as the distributions of ψ and θ within the specimens.

A relevant aspect that characterizes steady-state infiltration in

the centrifuge permeameter is that, for certain combinations of Q and ω, the ψ and θ in the upper portion of a specimen are relatively constant with height (Dell'Avanzi et al. 2004; Zornberg and McCartney 2010). Accordingly, for sufficiently high g levels, it is not necessary to measure θ and/or ψ throughout the entire specimen height. Instead, the average θ as measured by a TDR waveguide embedded within the wall of the permeameter is a good estimate of θ in the upper portion of the specimen (Zornberg and McCartney 2010). The θ measured with the TDR waveguide can be used to define the SWRC and K function, provided that the ψ and the K are also measured at midheight of the TDR waveguide (z_m=87 mm). The ψ at this height can be interpolated from the measurements from the tensiometers, which are located at heights of 23.5, 63.5, and 103.5 mm from the base of the permeameter.

Darcy's law can be used to define K for an unsaturated soil

$$K(\theta,\psi) = \frac{-v_m}{\frac{dh_e}{dz_m} + \frac{dh_p}{dz_m}} \quad (1)$$

where v_m=discharge velocity equal to the inflow rate divided by the cross-sectional area of the specimen and the denominator is the total hydraulic head gradient, equal to the sum of the gradients in centrifuge elevation head and water pressure heads. If the air pressure equals 0, the water pressure head gradient can be replaced by the suction head gradient, as follows:

$$\frac{dh_p}{dz_m} = -\frac{1}{\rho_w g}\frac{d\psi}{dz_m} \quad (2)$$

This term is negative as the ψ equals the difference between air pressure and water pressure. The centrifuge elevation head gradient is defined as

$$\frac{dh_e}{dz_m} = \frac{\omega^2}{g}(r_0 - z_m) \quad (3)$$

The centrifuge elevation head gradient equals the ratio between the centripetal acceleration at any height z_m from the base of the soil specimen and the acceleration due to normal earth gravity g, which is conventionally represented by the symbol N_r. The value of centrifuge elevation head gradient at midheight of the specimen $N_{r,\text{mid}}$ is referred to as the g level in this study.

K can be calculated from Eq. (1) through the control variables ω and Q, which are imposed values, along with the suction gradient $d\psi/dz_m$, which is defined using measured ψ values. It should be noted that K is a function of z_m because the two terms in the denominator of Eq. (1) are also functions of z_m. For consistency with the measured average θ, the expression for K, as well as the suction gradient, can be evaluated at the midheight of the TDR waveguide (z_m=87 mm).

For planning of a testing program, it is useful to define an approximate value of K that is only a function of the control variables. Specifically, at steady-state conditions, and assuming that the suction gradient is negligible in the upper portion of the specimen, the K in the specimen can be estimated to be K_{target} [see Eq. (11) in Zornberg and McCartney (2010)]. K_{target} values calculated for typical ω and Q values that can be used with the current centrifuge configuration range from 10^{-5} to 10^{-11} m/s under steady-state conditions, which is a reasonable range of K for unsaturated sands, silts, and clays of low plasticity.

The combination of the control variables ω and Q selected for a given test impacts the range of results, the testing time, and the total stresses on the specimen. Three approaches were evaluated in this study to reach the different K_{target} values needed to define the hydraulic characteristics of unsaturated soils: Approach (i) which involved imposing a constant ω and varying Q; Approach (ii) which involved imposing a constant Q and varying ω; and Approach (iii) which involved imposing varying values of both ω and Q. A schematic representation of the changes in control variables imposed on a soil specimen for testing Approaches (i), (ii), and (iii) is shown in Fig. 3(a). The arrows shown on each path indicate the succession of different test stages that would lead to changes in θ of a soil specimen.

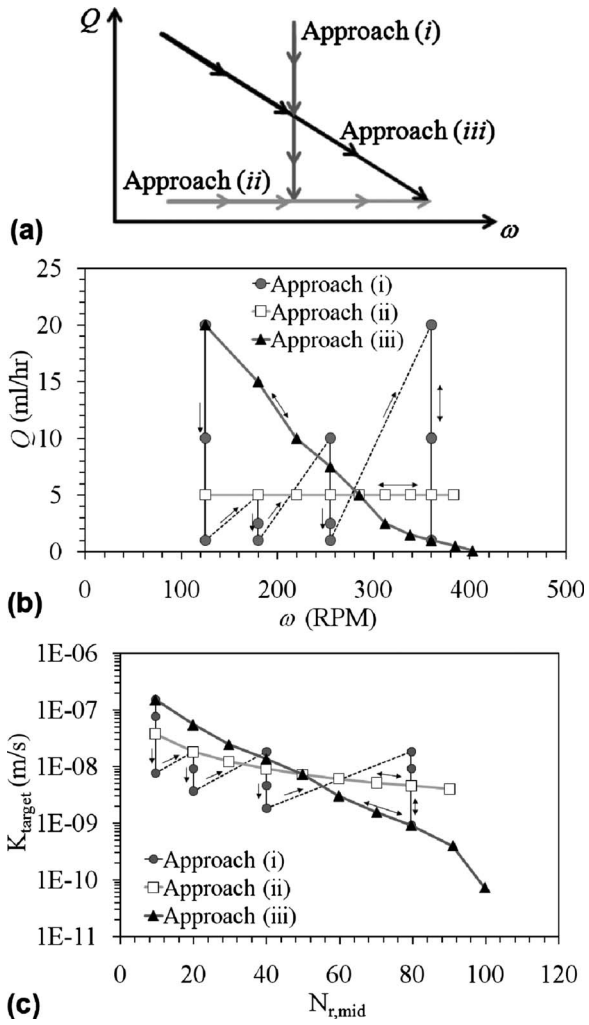

Fig. 3. Variation in control variables during different centrifuge permeameter testing approaches: (a) generic approaches used to evaluate drying paths of the hydraulic characteristics; (b) actual flow rates and angular velocities used in the three approaches; and (c) target K and g level values used in the three approaches. Note: Arrows indicate the direction of the tests. Dotted lines indicate transitions between different g levels for Approach (i).

In this study, a single test was performed on a pair of identical soil specimens in Permeameters A and B in three phases to evaluate the advantages and disadvantages of each testing approach and to assess the impact of both wetting and drying. The specific control variables, in terms of ω and Q, for each of the three test phases conducted in this study are shown in Fig. 3(b). The arrows denote the sequence of test stages during each test phase, and double-sided arrows indicate that both wetting and drying were evaluated. Approach (i) was evaluated in this test using four different angular velocities to evaluate the impact of g level on the

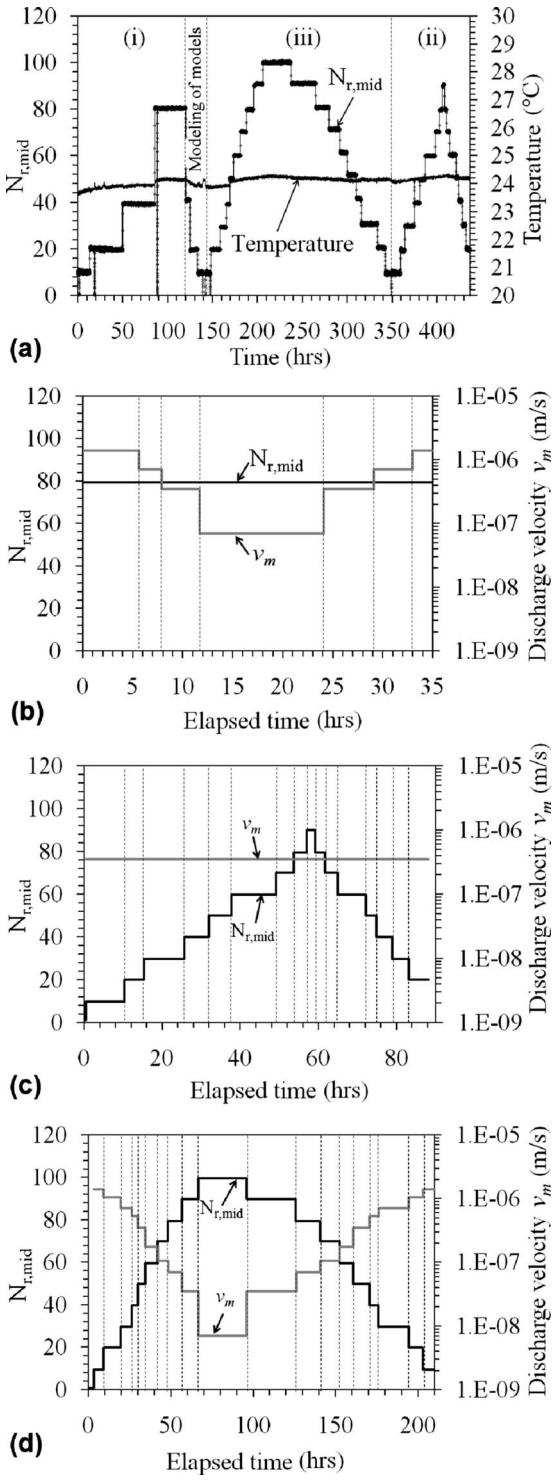

Fig. 4. (a) g level and permeameter temperature measurements during the centrifuge permeameter test; (b) g level and discharge velocity during the portion of the test focused on Approach (i); (c) g level and discharge velocity during the portion of the test focused on Approach (ii); and (d) g level and discharge velocity during the portion of the test focused on Approach (iii)

hydraulic characteristics determined using this approach. Tests using lower angular velocities were conducted first [see dashed lines with arrows in Fig. 4(b)]. The test phase conducted using Approach (ii) involved drying an initially saturated specimen by increasing ω in multiple stages while maintaining the same Q of 5 mL/h, followed by subsequent rewetting by reducing ω in multiple stages. The test phase conducted using Approach (iii) involved drying an initially saturated specimen by increasing ω and reducing Q in multiple stages, and subsequently retracing the changes in ω and Q to rewet the specimen. The same information shown in Fig. 3(b), but in terms of k_{target} and the g level $N_{r,mid}$, is shown in Fig. 3(c). The advantages and disadvantages of these approaches are discussed in detail later in this paper, but it should be noted from the paths in Fig. 3(c) that Approach (i) permits the definition of the hydraulic characteristics while subjecting the soil specimen to constant total stresses, while Approach (iii) provides the widest range of conditions to be used in the centrifuge permeameter.

Infiltration Results

A time series of the g level imposed during the centrifuge permeameter test is shown in Fig. 4(a), measured using the centrifuge g meter (a load cell attached to the permeameter frame). The vertical dashed lines show the four phases of testing conducted in this study. In this test, Approach (i) was evaluated first, a ramp-down phase was conducted subsequently (between the times of 120 and 142 h), in which different combinations of ω and v_m were applied to impose the same value of K_{target} on the specimen. Testing proceeded with an evaluation of Approach (iii) and finally of Approach (ii). The temperature measured during this test is also shown in Fig. 4(a), indicating that the temperature did not change significantly during centrifugation at different g levels. Only the last portion of the test phase in which Approach (i) was evaluated (i.e., at a g level of 80 g) involved both drying and subsequent rewetting. Consequently, the instrumentation results from only this portion of the first phase are shown for direct comparison with results obtained from the phases in which Approaches (ii) and (iii) were evaluated (they also involve drying and wetting). To facilitate discussion of the instrumentation results obtained during each of phase of the test described in Fig. 4(a), the elapsed times from the beginning of each phase [or from the time when a g level of 80 g was used in the evaluation of Approach (i)] are shown in the subsequent figures corresponding to each phase.

The time series for the target g level and discharge velocity (absolute value) imposed on both soil specimens during the evaluation of Approach (i) are shown in Fig. 4(b). The ratios between the values from these two time series [Eq. (11) in Zornberg and McCartney (2010)] for each stage equal the values of K_{target} shown in Fig. 3(c). During this phase, $N_{r,mid}$ was maintained constant while v_m was lowered in four stages, desaturating the specimens, and the specimen was rewetted by applying the same v_m but in the reverse order. The duration of each stage in this figure is a function of both the time required to reach steady-state conditions for a given combination of $N_{r,mid}$ and v_m, as well as of practical scheduling considerations during the multiday test. Stages with low v_m and low $N_{r,mid}$ generally require the longest time to reach steady-state conditions. At the end of each stage, the instrumentation results and imposed control variables are used to determine a point on the SWRC and the K function. The g level and discharge velocity for the phase in which Approach (ii) was evaluated are shown in Fig. 4(c). In this phase, the specimen was dried by increasing the g level in nine stages, and the specimen was subsequently rewetted in seven additional stages. The g level and discharge velocity for the phase in which Approach (iii) was evaluated are shown in Fig. 4(d). In this phase, the specimen was

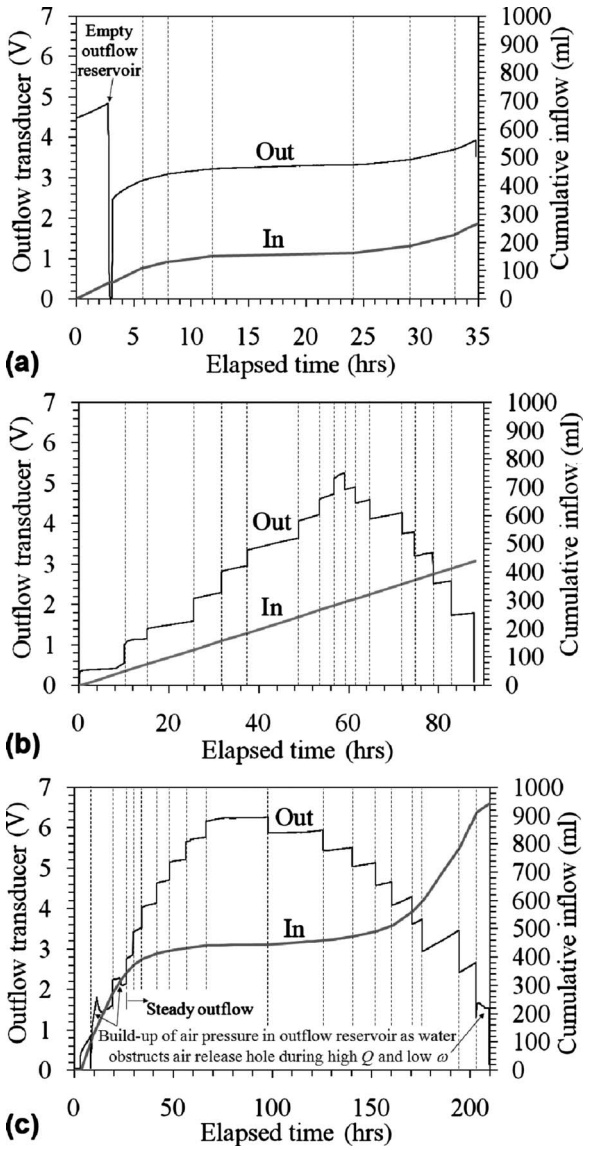

Fig. 5. Cumulative inflow and outflow transducer data: (a) Approach (i); (b) Approach (ii); and (c) Approach (iii)

initially dried in 10 stages, and the specimen was subsequently rewetted in nine additional stages.

The outflow transducer measurements along with the cumulative volume of imposed inflow are shown in Figs. 5(a–c) for the Approaches (i), (ii), and (iii) test phases, respectively. In these figures, outflow transducer measurements are shown in terms of millivolts, without using the calibrations presented by Zornberg and McCartney (2010) to define the outflow volumes. This facilitates showing the impact of g level on outflow measurements during the different approaches, showing when the centrifuge was stopped to empty the outflow reservoir. Also, outflow transducer measurements may potentially be affected by variables other than outflow of water (e.g., increased air pressure in the outflow reservoir if the air release hole becomes clogged). During any given test stage, the outflow is expected to increase nonlinearly until reaching steady-state conditions, when outflow should start following a linear trend with the same slope as that of the imposed inflow (Zornberg and McCartney (2010).

The outflow transducer readings from the Approach (i) test phase indicate that the pattern of outflow with time closely mirrors the cumulative inflow with time [Fig. 5(a)]. As this phase involved infiltration under a constant g level, no sharp changes are observed in the outflow transducer response. The only exception is at a time of 3 h, when the centrifuge was stopped to empty the outflow reservoir. The outflow transducer results from the Approach (ii) test phase show a shift in the transducer output at each change in the g level [Fig. 5(b)]. The inflow rate is constant during this approach so the cumulative infiltration follows a straight line. The slope of the outflow transducer reading in each stage is also relatively constant with time and consistent with that of the cumulative inflow. A minor difference in slope is observed because the slope of the calibration equation of the outflow transducer increases with g level. The outflow transducer results from the Approach (iii) test phase display a combination of the trends observed during the Approaches (i) and (ii) test phases [Fig. 5(c)]. Specifically, shifts in transducer output are noted due to changes in the imposed g level, while the slope of the outflow transducer voltage responses changes proportional to changes in the imposed inflow rate. During stages when low values of $N_{r,\text{mid}}$ and high values of v_m were imposed on the specimen [the first two and last stages in Fig. 5(c)], the outflow transducer showed voltage responses that were inconsistent with the trends in the imposed cumulative inflow. In addition, the voltage readings from the outflow transducers in Permeameters A and B, which are usually similar in trend, differed during these stages. This anomalous response could be explained by the high value of K_{target} (close to K_s), during these stages, which led to the high volumes of outflow from the specimen. Further, the g level may have been low enough to allow water migration from the outlet hole (the bottom support platen in the permeameter) to the air release hole, preventing air release [see Fig. 6(b) in Zornberg and McCartney (2010)]. This may have caused an increase in air pressure in the outflow reservoir, leading to a higher than expected voltage reading from the outflow transducer. Nonetheless, the data in Fig. 5(c) indicates that beyond a certain level of air pressure the water in the air release hole may have escaped reducing the air pressure, as shown by the subsequent voltage readings [e.g., around a time of 15 h in Fig. 5(c)]. After this point, the trends of outflow transducer readings are consistent with those of the imposed inflow.

The average θ values obtained from TDR measurements for Permeameter A from the Approach (i) test phase are shown in Fig. 6(a). A curve was fit to the data showing the data trend with time. A nonlinear trend in θ is observed at the beginning of each stage, although the θ reaches a stable value as steady-state conditions are established. McCartney (2007) found that TDR measurements for waveguides embedded in soil show an error of about 1%, although additional scatter in the TDR measurements could be expected during centrifuge testing due to the nonuniform θ along the length of the vertical waveguide during transient water flow. The θ measured during this test phase ranged from 26.1% (S_r=0.75) to 28.4% (S_r=0.81), which is a relatively narrow range due to the small range of K_{target} imposed in this test phase. ψ measurements from the three tensiometers during the Approach (i) test phase are shown in Fig. 6(b). Consistent with the θ measurement during this phase, changes in ψ are relatively minor. In fact, the ψ measured by the uppermost tensiometer remained nearly constant, with most of the changes occurring in the lower two tensiometer measurements. Tensiometer readings were influenced by changes in g level that occurred during stoppage of the centrifuge (to drain the outflow reservoir). This is due to the changes in self-weight of the water within the tensiometer reservoir at different g levels. Nonetheless, after restarting the centri-

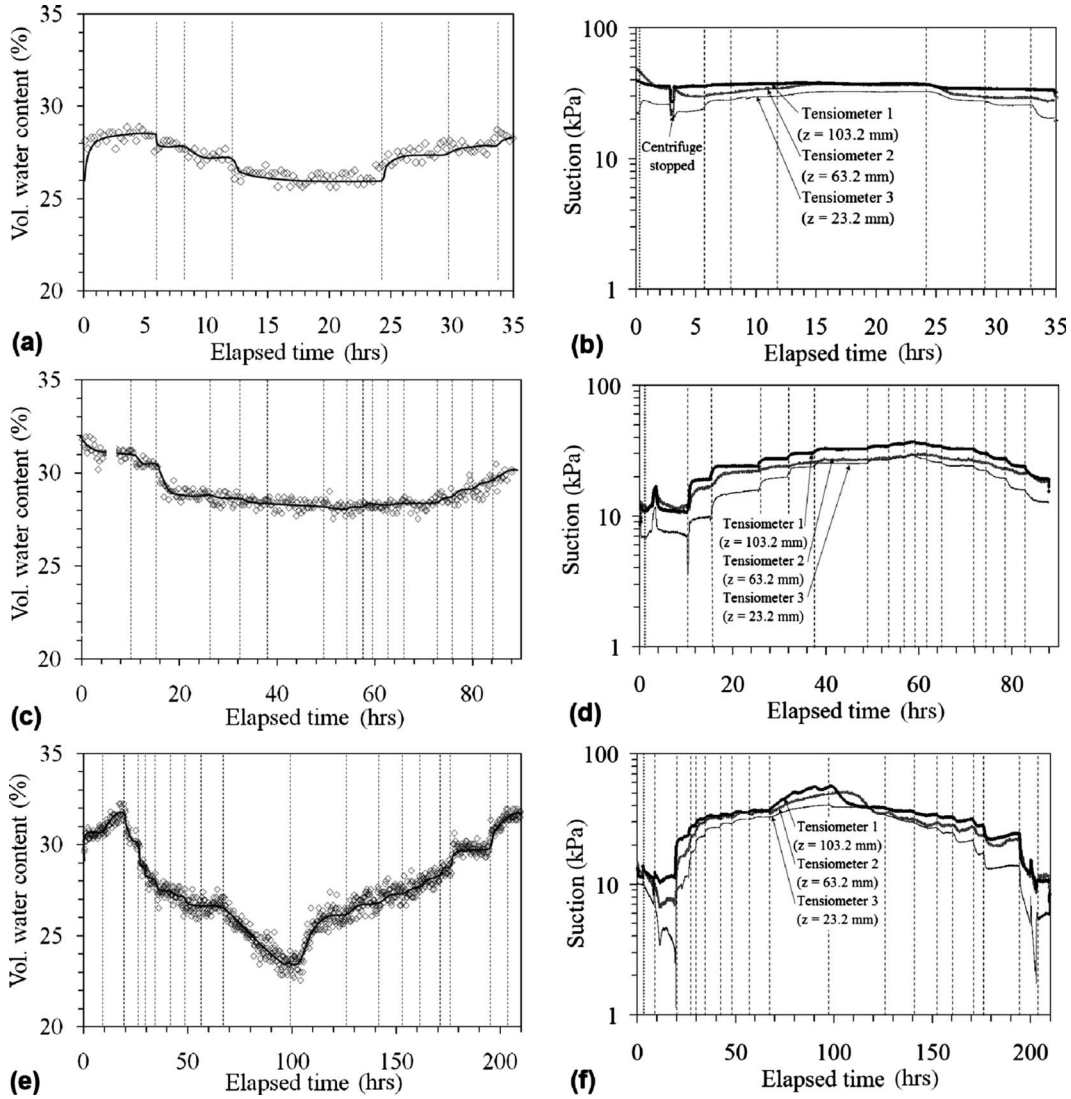

Fig. 6. (a) Average θ data obtained from the TDR waveguide during evaluation of Approach (i); (b) ψ data obtained from tensiometers at different depths in the permeameter during evaluation of Approach (i); (c) average θ data obtained during evaluation of Approach (ii); (d) ψ data obtained during evaluation of Approach (ii); (e) average θ data obtained during evaluation of Approach (iii); and (f) ψ data obtained during evaluation of Approach (iii)

fuge, the water pressure in the tensiometer re-equilibrated with the ψ in the soil.

The average θ values obtained from the Approach (ii) test phase are shown in Fig. 6(c). A wider range in θ values, ranging from 28% (S_r=0.80) to 31.2% (S_r=0.89), was obtained during this phase. The ψ measurements during this phase, shown in Fig. 6(d), also reflects a greater change in ψ than in the Approach (i) test phase due to a wider range in imposed K_{target} values. The scatter in the tensiometer measurements is less than that observed in TDR measurements, so the tensiometer data shows more clearly than the θ data the transient pattern that occurs during transitions from one stage to another. During each stage, ψ is observed to increase nonlinearly before reaching a constant value when steady-state flow is established. The top tensiometer (Tensiometer 1) reaches a constant value before the lower tensiometers during transitions from one stage to the next. An increase in ψ and a corresponding decrease in θ are noted during the first stage of this phase (elapsed time of 10 h), when the inflow was accidentally paused. Nonetheless, after reimposing the correct control variables the ψ and θ values returned to the conditions before inflow was paused.

The widest range of average θ values were obtained during the Approach (iii) test phase, as shown in Fig. 6(e). θ values ranged from 23.9% (S_r=0.68) to 31.8% (S_r=0.91). ψ results for this stage, shown in Fig. 6(f), also indicate the widest range in ψ among the three approaches. The highest ψ in Permeameter A observed in this phase was approximately 52 kPa, although a greater ψ of 70 kPa was measured in Permeameter B. During the second stage of this phase, the ψ decreased and the θ increased unexpectedly. It is possible that water could not exit from the base of the specimen due to the previously discussed buildup of air pressure [Fig. 5(c)]. Although steady-state flow conditions were observed in the outflow transducer readings toward the end of this stage, the θ data indicates that steady-state conditions were not reached. Accordingly, the results from this stage were not considered in the measurement of the soil hydraulic characteristics.

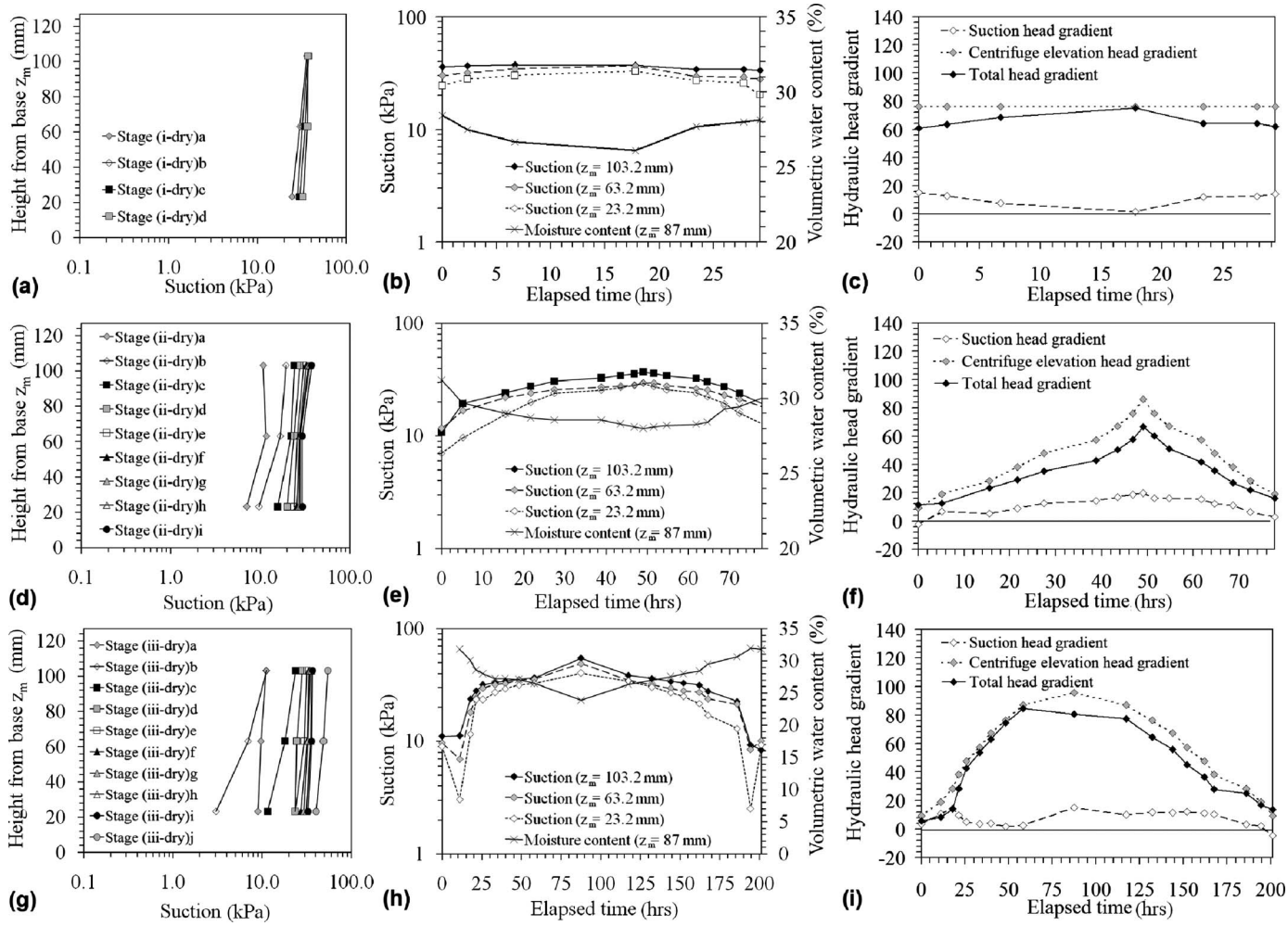

Fig. 7. Synthesized data from the infiltration test: (a) ψ profiles for the drying stages of Approach (i) test phase; (b) ψ and θ content results at steady-state conditions for Approach (i); (c) gradient values for Approach (i); (d) ψ profiles for the drying stages of Approach (ii) test phase; (e) ψ and θ results at steady-state conditions for Approach (ii); (f) gradient values for Approach (ii); (g) ψ profiles for the drying stages of Approach (iii) test phase; (h) ψ and θ results at steady-state conditions for Approach (iii); and (i) gradient values for Approach (iii)

Data Analysis

Synthesis of Instrumentation Results

The ψ profiles defined using the readings from the three tensiometers once steady-state conditions were established during the Approach (i) test phase are shown in Fig. 7(a). The profiles shown in the figure correspond to the results from the test stages in the drying portion of this phase, conducted by decreasing the inflow Q while maintaining the same angular velocity ω [labeled as Stages (i-dry)a, (i-dry)b, (i-dry)c, and (i-dry)d in the figure]. These ψ profiles show that the ψ was relatively constant in the upper portion of the specimen, which indicates that the θ along the TDR waveguide should be relatively constant for each test stage. The time histories for the ψ and θ values at steady-state conditions for each stage from both the drying and wetting portions of the Approach (i) test phase are shown in Fig. 7(b). While the changes in θ and ψ with time are not significant in this test phase, the θ and ψ trends are consistent throughout the test phase (*i.e.*, decreasing θ values correspond to increasing ψ). Finally, the suction head gradients calculated using the tensiometer measurements [Fig. 7(b)] and Eq. (2), the centrifuge elevation head gradient calculated using the control variables and Eq. (3), and their sum (the total head gradient), are shown in Fig. 7(c) for the same test phase. The suction head gradient values are significantly smaller than the centrifuge elevation head gradients throughout the entire test phase. The suction head gradient is greater for test stages in which the value of K_{target} was close to K_s (i.e., low $N_{r,\text{mid}}$ and high v_m).

Similar information is shown in Figs. 7(d–f) to that shown in Figs. 7(a–c), but for the Approach (ii) test phase. During this phase, the ψ profiles show a greater difference between the ψ values measured at the top and bottom of the specimen, especially for stages conducted at low g levels. This phase was evaluated last in the sequence of phases shown in Fig. 4(a). Consequently, the soil samples were dissected in five layers after completion of the testing program for measurement of the final gravimetric θ profile using oven drying. The results, reported by McCartney (2007), indicate that the θ profile was consistent with that obtained from the ψ profile measured using the tensiometers. Finally, Figs. 7(g–i) show the same information as shown in the previous figures, but for the Approach (iii) test phase. During this phase, the ψ profiles reach higher values as the values of imposed

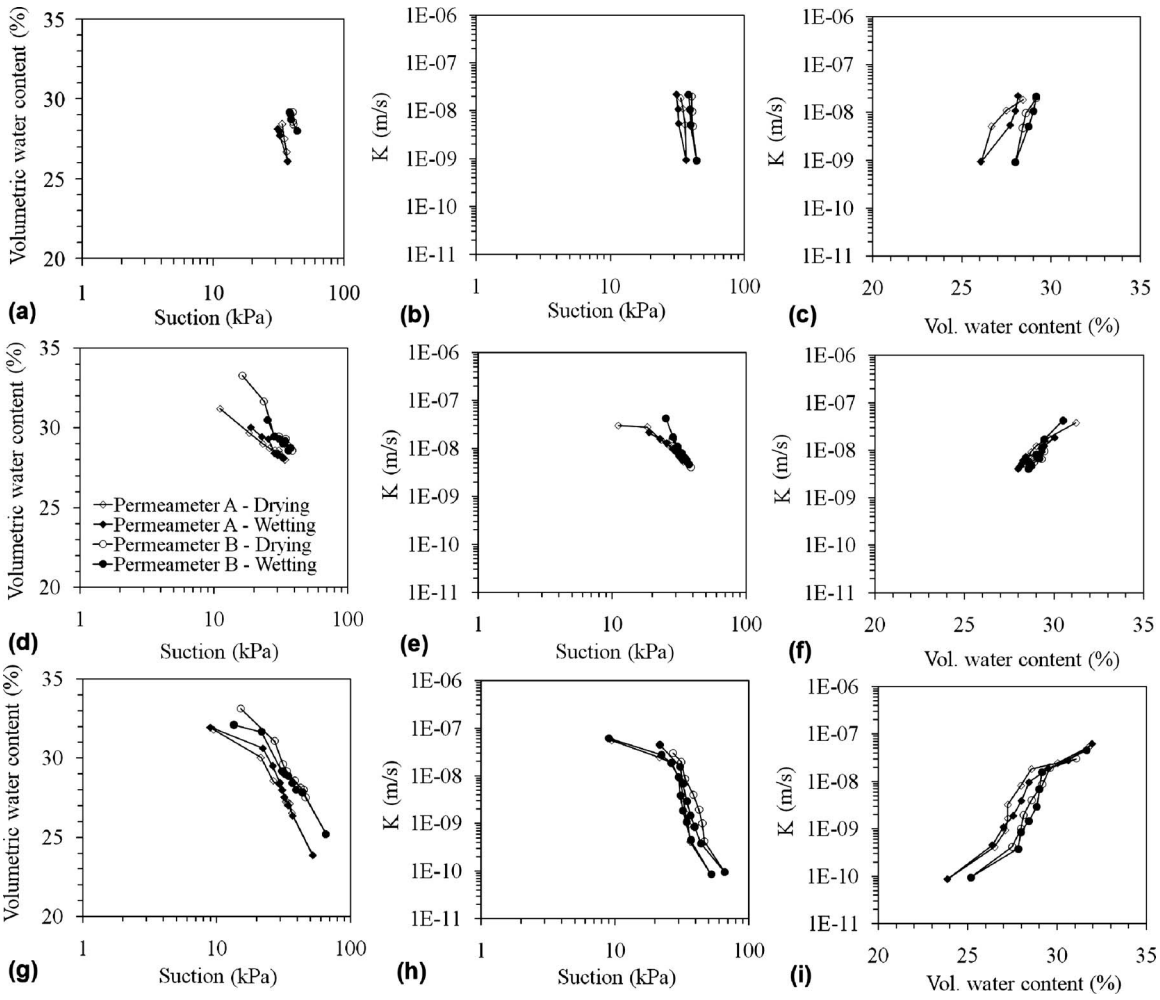

Fig. 8. Hydraulic characteristics: (a) θ-ψ Approach (id); (b) *K*ψ Approach (id); (c) *K*-θ Approach (id); (d) θ-ψ Approach (ii); (e) *K*-ψ Approach (ii); (f) *K*-θ Approach (ii); (g) θ-ψ Approach (iii); (h) *K*-ψ Approach (iii); and (i) *K*-θ Approach (iii)

K_{target} were decreased during subsequent stages. In addition, ψ became more uniform with height in the specimen from stage to stage in the drying portion of this phase, as the *g* level was increased and the infiltration rate was decreased.

Consistent with observations from solutions to Richards' equation (Zornberg and McCartney 2010), the shapes of the ψ profiles suggest that the value of ψ at the bottom outflow boundary of the specimen does not impact the value of ψ in the upper portion of the specimen. The zone of soil affected by the bottom boundary condition is small, which is consistent with the concept of "open-flow centrifugation" proposed by Conca and Wright (1992). Unlike the pattern observed in the ψ profile during steady-state infiltration under high *g* levels, the pattern observed during steady-state infiltration using the same soil but in a 1-g column test showed a significant increase in θ near the bottom boundary, consistent with the zone of nonuniform ψ observed by McCartney and Zornberg (2007). The differences between the centrifuge permeameter and 1-g column results can be explained by the decreased region with a nonuniform ψ value obtained for increased *g* levels (Dell'Avanzi et al. 2004).

Measurement of Hydraulic Characteristics

The ψ and θ data at steady-state conditions at the end of each stage shown in Fig. 7(b) were synthesized to determine the SWRC obtained using Approach (i), as shown in Fig. 8(a). In addition, the SWRC defined using the instrumentation results from Permeameter B are shown in this figure. The results shown in this figure indicate that a relatively small portion of the SWRC could be defined using this approach. The steep change in θ with slight changes in ψ suggests that the ψ values obtained during this phase correspond to a range of the SWRC beyond the air-entry suction. The wetting and drying paths are similar, indicating negligible hysteresis. This may be due to the fact that wetting and drying paths observed in this study are scanning curves (i.e., the infiltration test did not start with a specimen having $S_r=1$). Nonetheless, the lack of hysteresis may also be due to the fact that steady-state infiltration was used to define different values on the SWRC, implying that the likelihood of air entrapment was decreased.

The *K* results for Permeameters A and B, plotted against the ψ values measured at steady-state conditions, are shown in Fig. 8(b). For the specimens in both permeameters, a decrease in *K* of two orders of magnitude (i.e., from 2.3×10^{-8} to 9.3×10^{-10} m/s) was observed for a change in ψ of approximately 3 kPa. Also in this case, relatively little hysteresis was noted in the *K*-ψ relationship. The same decrease in *K* is observed in Fig. 8(c) but for a change in θ of approximately 2%. Although slight hysteresis was noted for the specimen in Permeameter A, this could

still be considered minor. The relatively narrow shapes of the hydraulic characteristics shown in Figs. 8(a–c) are due the relatively small range of K_{target} values imposed on the specimen.

Similar information to that shown in Figs. 8(a–f) is shown in Figs. 8(d–f), respectively, but for Permeameters A and B from the Approach (ii) test phase. The SWRC obtained using Approach (ii) has a wider range in ψ values (31 to 39 kPa), which corresponds to a wider range in average θ values (28.0 to 33.3%). Lower K values were measured using this approach (3.0×10^{-8} to 5.2×10^{-9} m/s) than in Approach (ii). The hydraulic characteristics measured for the soil specimens in both permeameters were similar, although the specimen in Permeameter B was wetter at the beginning of this phase. Consistent with the hydraulic characteristics obtained using Approach (i), negligible hysteresis was noted in the data.

The SWRC obtained using Approach (iii), shown in Fig. 8(g), show the widest range in ψ (9 to 66 kPa) and the widest range in θ (23 to 33%) because high g levels and low discharge velocities simultaneously. The K functions plotted as functions of ψ and θ in Fig. 8(h and i), respectively, show a four orders of magnitude decrease in K (6.2×10^{-7} to 8.7×10^{11} m/s) during the drying portion of this phase. The results obtained for the soil specimens in both permeameters follow the same shape, although the θ in the Permeameter B specimen was consistently higher for the same ψs values. This is likely due to the slight difference in porosity of the specimen (34.9% for the specimen in Permeameter A, and 34.3% for the specimen in Permeameter B).

The lack of hysteresis observed in the hydraulic characteristics is possibly due to the relatively narrow range of θ values evaluated in this study. Specifically, the specimen was desaturated to θ values at which the volumetric air content exceeded 32%, so it is less likely that air would be entrapped in the soil pores during rewetting, which has been explained as a cause of hysteresis (Topp and Miller 1966). It is also possible that the lack of hysteresis is due to the fact that steady-state water flow was used in this study. As water flow was never stopped during this test, water may have flowed through the same pore pathways in during both wetting and drying. Another interesting observation of the hydraulic characteristics measured in this study is that the hysteresis was negligible in the K function regardless of whether it was plotted as a function of θ or ψ. This contradicts observations by Topp and Miller (1966), who found that hysteresis was more prominent in the K-ψ relationship than in the K-θ relationship. It may be speculated that the measured hysteresis is a product of the transient nature of previous experimental studies, but that such hysteresis may only be temporary and, ultimately does not occur once steady-state flow conditions are reached. Another possible reason that hysteresis was not noted in the text is that the wetting and drying curves measured in this study are scanning curves (i.e., the test was not started from 100% saturated conditions) (Topp and Miller 1966). However, these scanning curves are representative of real wetting and drying processes during infiltration in field situations.

Evaluation of Results

Effect of g Level on the Definition of the SWRC and K Function

One of the phases of the test shown in Fig. 4(a) was performed to verify that the same results can be obtained for different g levels, provided that the imposed flow rate is varied accordingly.

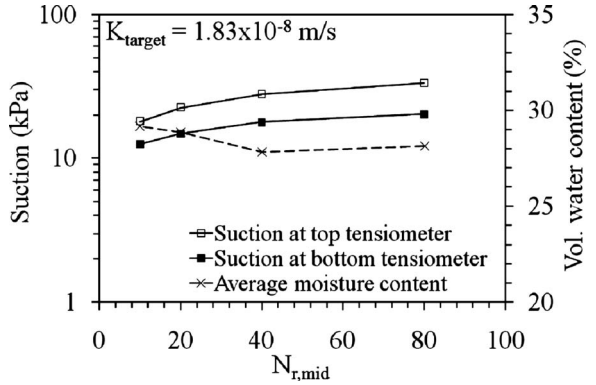

Fig. 9. ψ and θ values at steady-state flow under different combinations of ω and v_m leading to the same K_{target} values

During this phase, different values of g level and discharge velocity were adopted in four stages to reach the same value K_{target} of 1.8×10^{-8} m/s in the specimen. The θ and ψ values measured in the specimen in Permeameter A at steady-state conditions during the each of the four stages in this phase are shown in Fig. 9. Similar results for Permeameter B were noted. The θ and ψ values for an imposed K_{target} value approach a constant value for increasing g levels. This is consistent with observations from theoretical solutions to Richards' equation in the centrifuge, which suggest that the ψ profile becomes more uniform with height for increasing g levels. The calculated values of K using the measured ψ data shown in Fig. 9 and Eq. (1) are only slightly greater than K_{target} value, with the difference decreasing with increasing g level (e.g., K for Permeameter A is 2.25×10^{-8} m/s at g levels of both 40 and 80, but is 2.43×10^{-8} m/s at g level of 10). The comparatively higher K at lower g levels is consistent with the comparatively higher θ values and lower ψ values shown in Fig. 9 for lower g levels.

In addition to the hydraulic characteristics obtained using Approach (i) and shown in Figs. 8(a–c), which included wetting and drying curves at $N_{r,mid}$=80 g, drying curves were also obtained using g levels of 10, 20, and 40 g. Comparison of the drying curves from all four of these approaches permits assessment of any impact that the g level (and consequently the total stress on the specimens) may have on the hydraulic characteristics. The SWRCs from these four g levels using Approach (i) are shown in Fig. 10(a). The θ follows the same trend with increasing ψ, although there is some scatter due to the large rewetting transition periods [when the K_{target} values at the end of infiltration at each g level were increased to initiate testing at the next g level, see Fig. 3(b)]. Although the results from each g level span over wide ranges of θ, ψ, and K, data points used to define the K functions in Figs. 10(b and c) follow the same trends. The K at saturation and the porosity are shown in these figures for reference, although it should be noted that the ψ is on a logarithmic scale and does not extend to saturation. The results in Fig. 10, along with the fact that negligible settlement was noted in the specimens in Permeameters A and B at the end of the test suggest that the increased g level (and total stresses) imposed during centrifuge testing did not affect the SWRC and K function of the compacted clay evaluated in this study.

Comparison of Measured Results with Those from Predictive Relationships

The data from the drying paths of the SWRCs determined the three approaches, for the soil specimens in Permeameters A and

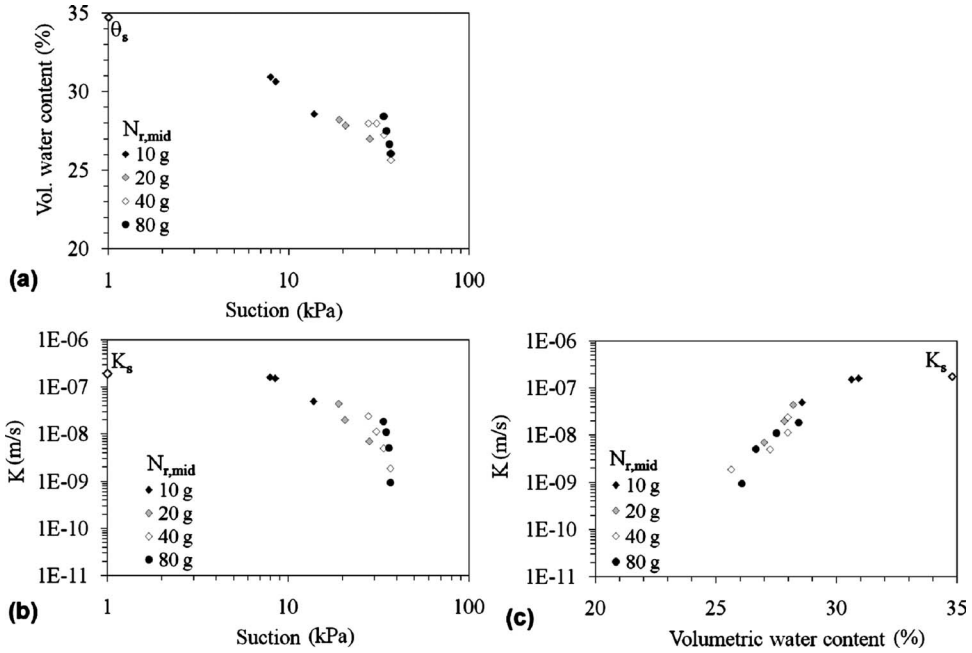

Fig. 10. Comparison of hydraulic characteristics obtained under different g levels from Permeameter A: (a) θ-ψ; (b) K-ψ; and (c) K-θ

B, are shown in Fig. 11(a). The data from all three approaches appear to define a single relationship, following a nonlinear decreasing trend. The van Genuchten (1980) model was fitted to both sets of data with parameters shown in the figure. The actual porosity values of 34.9% for Permeameter A and 34.3% for Permeameter B along with a residual θ of 5% were also used in the fitting. The porosity values for both specimens are shown for reference, although these SWRC data points cannot be rigorously shown when using a logarithmic scale. Comparison of the data with the fitted curves suggests that the range of ψ obtained in the specimen was beyond the air-entry suction of the soil, providing data points to define the downward slope of the desaturation portion of the van Genuchten (1980) model. The K functions in terms of ψ are shown in Fig. 11(b), along with the K function predicted using the van Genuchten-Mualem (van Genuchten 1980) model. The K_s value is also shown for reference. The predicted K function for the Permeameter A specimen indicates that the K at a ψ of 1 kPa is 3 times smaller than K_s due to the comparatively steep slope of the SWRC for the Permeameter A specimen at small values of ψ [see Fig. 11(a)]. Although the model appears to predict the correct slope of the K function for ψ values below 20 kPa, the experimental data and predicted curve deviate significantly at

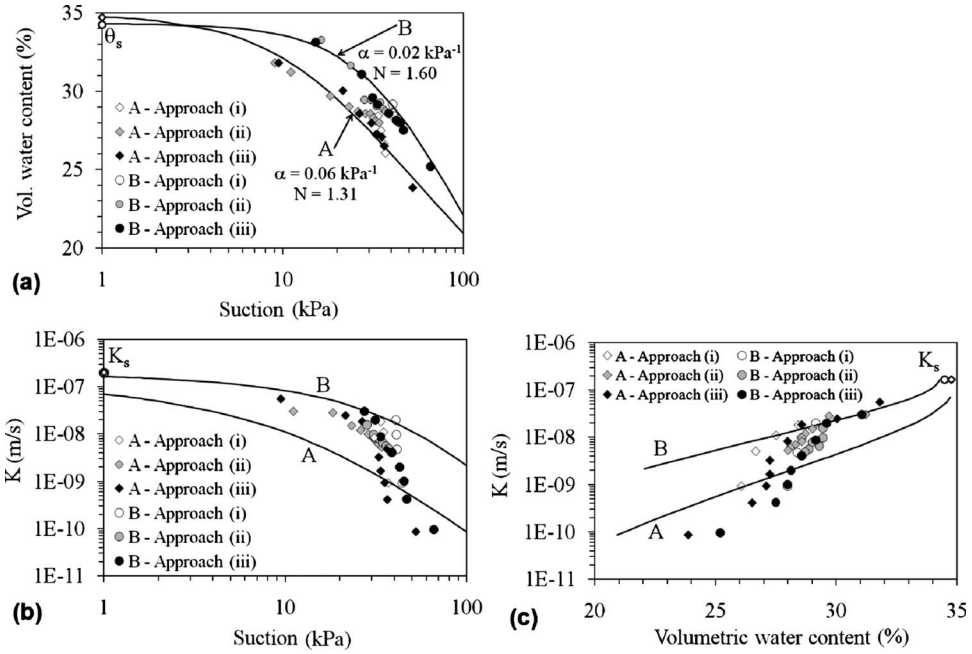

Fig. 11. Comparison of the hydraulic characteristics measured in Permeameters A and B with the van Genuchten-Mualem (van Genuchten 1980) model: (a) θ-ψ with fitted SWRC; (b) K-ψ with predicted K function; and (c) K-θ, with predicted K function

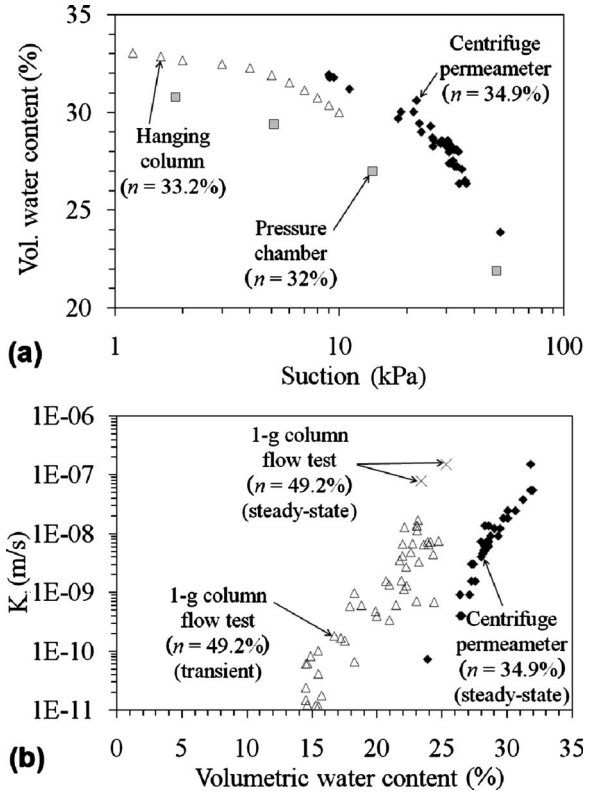

Fig. 12. Comparison of hydraulic characteristics from the centrifuge permeameter with those from conventional tests: (a) θ-ψ; (b) *K*-θ

higher values of ψ. In fact, the experimental and predicted curves deviate by nearly four orders of magnitude at a ψ of 76 kPa for the specimen in Permeameter B. Similar observations can be made from inspection of the *K* functions represented in terms of θ, as shown in Fig. 11(c). The predicted *K* functions show a good match with the experimental data at high θ values, but deviate as for low θ values. Even if the predicted *K* function were scaled linearly to a *K* value other than K_s, as suggested by Khaleel et al. (1995), the predicted *K* function would not provide a good fit.

The poor match of the experimental and predicted *K* function emphasizes the importance of determining the *K* function experimentally rather than relying on predictive relationships. The *K* functions determined using the centrifuge permeameter provide enough data to characterize the slope of the *K* function using a log-linear function such as that proposed by Gardner (1958). McCartney (2007) found that the *K* functions shown in Fig. 11(b) are well represented by a log-linear function with a slope of 0.11 kPa^{-1} (i.e., Gardner's α parameter) for ψ values greater than 10 kPa. For ψ values below 10 kPa, the *K* can be assumed equal to K_s.

Comparison of Centrifuge Results with Those from Conventional Approaches

A comparison between the SWRCs determined using centrifuge test results (for the Permeameter A specimen) with those determined using other approaches described in ASTM D6836 (ASTM 2001), including the pressure chamber and hanging column tests, is shown in Fig. 12(a). Unlike the *K* function, which is usually defined using predictive relationships in engineering practice, experimental SWRCs determined using the hanging column and pressure chamber tests are typically used with confidence. Although the porosities of the soil specimens evaluated using these different approaches are different [see porosity values in Fig. 12(a)], the shape of the SWRC defined using the centrifuge and conventional approaches is the same for the range of ψ shown in the figure. The α and *N* parameters from the van Genuchten (1980) model are similar for the data from all three different tests, although with different porosity values. The good agreement among between the shapes of the SWRCs validates the adequacy of the results obtained using the new centrifuge permeameter.

A comparison between the *K* function obtained from a 0.75-m-long, 1-g column flow test on the same soil used in this study (McCartney et al. 2007) with the *K* function obtained from the centrifuge permeameter is shown in Fig. 12(b). The *K* values from the 1-g column flow test were determined using a steady-state approach similar to that used in this study. Specifically, the length of the soil layer in the column test was 0.75 m, which was sufficient to permit the development of a "unit-gradient" zone in the upper portion of the column, where the ψ and θ were uniform. For these conditions, the *K* in the 1-g column test was determined with $N_{r,\mathrm{mid}}=1$. However, approximately 1,200 h were required to reach steady-state flow for two different discharge velocities, which permitted only two points on the *K* function to be determined using this approach. Accordingly, the *K* was also determined using the instantaneous profile method, which involves interpretation of the transient changes in θ during infiltration (Olson and Daniel 1981). The results from both analyses of the 1-g column test are shown in Fig. 12(b). The porosity of the soil evaluated in the column test was 49.2% and K_s was equal to 6.6×10^{-6} m/s. Despite these different soil conditions, the results obtained from the 1-g column flow test follow the same trend as those obtained from the centrifuge test. Accordingly, this comparison provides evidence of the validity of the centrifuge permeameter results. It should be noted that the centrifuge permeameter results show significantly less scatter than those obtained from the transient analysis in the 1-g column flow test, suggesting that the use of steady-state infiltration permits a more confident estimate of the shape of the *K* function.

Evaluation of Testing Times

A major advantage of using the centrifuge permeameter to determine the SWRC and *K* function of soils is that steady-state conditions can be reached in a shorter period of time than that required in 1-g tests (e.g., column inflow tests). This is because a uniform ψ profile can be established in a relatively short centrifuge specimen (126 mm), so the time requirements for flow across the specimen are much less than in a geometrically equivalent soil column under 1-g conditions. The factors that affect the time required to reach steady-state water flow during centrifuge test stage include the magnitude of change in the imposed flow rate from a previous test stage (faster for higher inflow rates), the magnitude of the *g* level (faster for higher *g* levels), the response time of the tensiometers, and whether testing involved wetting or drying paths (faster for drying). Evaluation of the ψ data in Fig. 6(f) for the Approach (iii) test phase indicates that wetting requires more time to reach equilibrium, likely because the tensiometers require a longer time to equilibrate for wetting than for drying. Among the factors listed above, the testing time was found to be extended the most by the transition period required to change inflow rates from stage to stage. Approaches (i) and (iii) required longer testing times than Approach (ii) as they require equilibration under a new inflow rate at each intermediate testing

stage. For example, the tensiometer results in Figs. 7 and 6(b and f) indicate that the stages with low infiltration rates required the longest times to reach steady-state conditions.

As mentioned in the previous section, only two points on the K function could be obtained using 1-g steady-state infiltration after nearly 1,200 h of infiltration. Additional perspective on the time savings of the centrifuge approach can be gained by evaluating conventional scaling laws (Cargill and Ko 1983). Specifically, length scales linearly and time scales quadratically in the flow process involved in the centrifuge permeameter. For example, a 0.75-m-long soil column could be modeled using the 126-mm-long centrifuge permeameter during infiltration at a g level of 6. In this case, the 1,200 h test under 1 g could be completed after $1{,}200/36=3$ h under 6 g. Although at test under 6 g was not conducted in this study, only 12 h were required to reach steady-state conditions during inflow under 10 g using Approach (ii) [see Fig. 4(c)]. This emphasizes the expeditious nature of centrifuge permeameter tests compared to conventional tests.

Conclusions

The following conclusions may be drawn from the tests performed in this study to determine the SWRC and hydraulic conductivity function (K function) of a clay of low plasticity using steady-state infiltration in a centrifuge permeameter:

- Measured ψ profiles were consistent with those expected from theoretical analyses of steady-state infiltration. Specifically, the ψ profiles in the centrifuge permeameter measured using tensiometers, as well as gravimetric water content samples, indicate that ψ and θ are uniform in the upper portion of the soil specimen during steady-state infiltration in the centrifuge. The ψ profile was observed to be more uniform with height in the specimen as the g level increases and as the inflow rate decreases.
- Uniformity of the ψ profile supports the use of a K value defined by assuming that the suction gradient is negligible (i.e., K_{target}) to define the testing program. This is commonly used in other centrifuge permeameter approaches in which ψ is not measured during centrifugation.
- The centrifuge permeameter was successfully used as a new device for measurement of the hydraulic characteristics of unsaturated soils. In particular, for a compacted clay of low plasticity tested under a range of inflow rates (20 to 0.1 mL/h) and centrifuge speeds (100 to 400 rpm), ψ values ranged from 5 to 70 kPa, average volumetric water content values ranged from 23 to 33%, and K values ranged from 2×10^{-7} to 8×10^{-11} m/s. Application of lower K values is possible, although a different suction measurement approach may be necessary. Nonetheless, the centrifuge permeameter tests provide sufficient data to characterize the slope of the K function using a log-linear function.
- Negligible hysteresis was observed in the hydraulic characteristics obtained using steady-state infiltration.
- The use of different combinations of inflow rate and centrifuge speed for characterization was observed to lead to essentially the same SWRC and K function for the compacted soil evaluated in this study. Nonetheless, a testing approach that involves increasing the centrifuge speed and decreasing the inflow rate in stages was found to provide the most amount of data in the shortest test duration.
- Because the soil investigated in this study was compacted, the changes in total stresses associated with application of different g levels during centrifuge permeameter testing did not lead to settlement or a change in the SWRC or K function. In-flight displacement measurements would be needed for testing of compressible soils to account for volumetric changes.
- Comparison of results from nearly identical soil specimens tested concurrently in the centrifuge indicated good repeatability of results.
- The hydraulic characteristics obtained using the centrifuge permeameter are consistent with those obtained using conventional techniques. However, centrifuge test results were obtained in significantly less time than in conventional tests (e.g., 200 h were needed to determine 20 points in the centrifuge permeameter versus 1,800 h needed to obtain 2 points under steady-state conditions in a 1-g column infiltration test). Less scatter was observed in the experimental SWRC and K function obtained using steady-state infiltration in the centrifuge permeameter than in the SWRC defined by analysis of transient inflow data in 1-g column infiltration tests.
- The K functions defined using the centrifuge permeameter follow the same shape as those obtained from predictive relationships, although the measured and predicted K functions differ by two orders of magnitude at the lower end of the volumetric water content range. This emphasizes the importance of determining the K function experimentally rather than relying on predictive relationships.

Acknowledgments

Support received from the National Science Foundation under Grant No. CMS-0401488 is gratefully appreciated.

References

ASTM. (2000). "Standard test method for determining unsaturated and saturated hydraulic conductivity in porous media by steady-state centrifugation." *ASTM D6527*, West Conshohoken, Pa.

ASTM. (2001). "Standard test methods for determination of the soil water characteristic curve for desorption using a hanging column, pressure extractor, chilled mirror hygrometer, and/or centrifuge." *ASTM D6836*, West Conshohocken, Pa.

Cargill, K. W., and Ko, H.-Y. (1983). "Centrifugal modeling of transient water flow." *J. Geotech. Engrg.*, 109(4), 536–555.

Conca, J., and Wright, J. (1992). "Diffusion and flow in gravel, soil, and whole rock." *Applied Hydrogeology*, 1, 5–24.

Dell'Avanzi, E., Zornberg, J. G., and Cabral, A. (2004). "Suction profiles and scale factors for unsaturated flow under increased gravitational field." *Soil Found.*, 44(3), 1–11.

Gardner, W. (1958). "Some steady-state solutions of the unsaturated moisture flow equation with applications to evaporation from a water table." *Soil Sci.*, 85, 228–232.

Khaleel, R., Relyea, J., and Conca, J. (1995). "Evaluation of van Genuchten-Mualem relationships to estimate unsaturated hydraulic conductivity at low water contents." *Water Resour. Res.*, 31(11), 2659–2668.

McCartney, J. S. (2007). "Determination of the hydraulic characteristics of unsaturated soils using a centrifuge permeameter." Ph.D. dissertation, Univ. of Texas at Austin, Austin, Tex.

McCartney, J. S., Villar, L., and Zornberg, J. G. (2007). "Estimation of the hydraulic conductivity function of an unsaturated clay using an infiltration column test." *Proc., 6th Brazilian Conference on Unsaturated Soils (NSAT)*, UFBA, Salvador, Bahia, Brazil.

McCartney, J. S. and Zornberg, J. G. (2007). "Effect of wet-dry cycles on

capillary break formation in geosynthetic drainage layers." Geosynthetics 2007, Washington, D.C.

Nimmo, J., Rubin, J., and Hammermeister, D. (1987). "Unsaturated flow in a centrifugal field: Measurement of hydraulic conductivity and testing of Darcy's law." *Water Resour. Res.*, 23(1), 124–134.

Olson, R., and Daniel, D. (1981). "Measurement of the hydraulic conductivity of fine grained soils." *Permeability and groundwater contaminant transport, ASTM STP746*, T. F. Zimmie and C. O. Riggs, eds., ASTM, West Conshohoken, Pa., 18–64.

Topp, G. C., and Miller, E. E. (1966). "Hysteretic moisture characteristics and hydraulic conductivities for glass-bead media." *Soil Sci. Soc. Am. J.*, 30, 156–162.

van Genuchten, M. (1980). "A closed-form equation for predicting the hydraulic conductivity of unsaturated soils." *Soil Sci. Soc. Am. J.*, 44, 892–898.

Zornberg, J. G., and McCartney, J. S. (2010). "Centrifuge permeameter for unsaturated soils. I: Theoretical basis and experimental developments." *J. Geotech. Geoenviron. Eng.*, 136(8), 1051–1063.